LOW-DISPERSION TURNS FOR MICRO CE SYSTEMS

Guan-Liang Chang*, Lung-Ming Fu**, Chia-Yen Lee***, Che-Hsin Lin****, Chien-Hsiung Tsai*****

*Institute of Biomedical Engineering, National Cheng-Kung University, Tainan, Taiwan
**Graduate Institute of Materials Engineering
National Pingtung University of Science and Technology, Pingtung, Taiwan
***Department of Mechanical and Automation Engineering, Da-Yeh University, Taiwan
****Department of Mechanical and Electro-mechanical Engineering,
National Sun Yat-sen University, Kaohsiung, Taiwan
*****Department of Vehicle Engineering,
National Pingtung University of Science and Technology, Pingtung, Taiwan

loudyfu@mail.npust.edu.tw, cy@mail.dyu.edu.tw, chehsin@mail.nsysu.edu.tw and
chtsai@mail.npust.edu.tw

Abstract : This paper performs numerical and experimental investigations into the influence of the geometric bend ratio on turn-induced dispersion within U-shaped separation channels. The separation efficiency of an electrophoresis microfluidic device is known to be influenced significantly by the geometry and flow field conditions of the separation microchannel. Consequently, developing a thorough understanding of the effects of different geometries on the flow field physics in the separation microchannel is of fundamental concern in improving the design and operation of microfluidic chipsystems. The turns in a microfabricated separation channel tend to induce a band-broadening effect which degrades the separation efficiency of the device. Consequently, the present study designs and tests various geometric bend ratios with the aim of reducing this so-called "racetrack" effect. A good agreement is obtained between the numerical and experimental results. It is shown that the serpentine U-shaped channel configuration is ideally suited to the efficient separation of this sample within miniature microfluidic devices.

Introduction

Microfluidic electrophoresis [1] is commonly employed in applications requiring the separation of biological or chemical particles. The capillary electrophoresis technique exploits the differing mobility characteristics of charged molecular species under the influence of an external electric field. Electroosmotic flow is a bulk flow of solution resulting from movement induced in the double layer at the capillary surface by the application of this electric field. Under typical capillary electrophoresis conditions, the electroosmotic flow travels from the positive to the negative electrode. Meanwhile, negatively charged species undergo electrophoretic migration in the opposite direction. In both cases, however, the overall direction of the charged species is given by the sum of the electrophoretic and electroosmotic velocities.

The injection and separation channels of a microfluidic device are generally configured within a very compact area of the microfabricated chip. Such microfluidic chips typically employ electrokinetic manipulation techniques to handle and analyze the fluid. Previous researchers have demonstrated that by coupling the chips with other analytical techniques such as cell injection and cell lysis [2], it is possible to construct an integrated chemical analysis system which satisfies the Lab-on-a-Chip concept, e.g. polymerase chain reaction-capillary electrophoresis (PCR-CE), cell sorting-counting[3], mixer-capillary electrophoresis, and various other analysis devices[4].

Since the electrophoresis separation microchannels are generally designed within a compact area of the microfabricated chip, it is necessary to utilize a serpentine channel configuration if the required separation length is to be achieved. In attempting to increase electrophoresis separation efficiency while simultaneously decreasing product cost and enhancing device miniaturization, researchers have recently investigated a variety of different serpentine microchannel configurations. Turn-induced band broadening has been linked directly to the angle of the turn and to the width of the separation channel. Culbertson *et al.* [5] demonstrated that constant radius corners increase the sample dispersion of flows within electrokinetic microchannels, and therefore offset the benefits accruing from the additional separation length. The stretching of the analytical band as it traverses a turn in the microchannel is commonly referred to as the "racetrack effect". Their results indicated that a bend ratio of 4:1 corrected band tilting in the detection area

ISSN: 1727-1983

and reduced the racetrack effect. Molho *et al.*[6] employed simulation techniques to design and test a novel compensating corner geometry which reduced the racetrack effect induced in the serpentine electrophoretic separation channels in microchips. Recently, various researchers have employed the compelling method of control the zeta potential to reduce turn-induced spreading in serpentine microchannels. The current study utilizes experimental and numerical methods to develop an optimal serpentine channel geometry which minimizes turn-induced dispersive spreading. Photographs of the current serpentine U-shaped separation channels are presented in Figure 1. It is noted that two separate microfluidic devices are shown in Figure 1(a). Although the total length of the separation channel is 3 cm in both cases, the bend ratios are different. In Figure 1(b), the bend ratio is 1, whereas in Figure 1(c), the bend ratio is 4. The current study develops analytical models to characterize constant radius turns, serpentine channels comprising dispersion-inducing turns, and flow fields within serpentine channels. Through simulation and experimental investigations, this study attempts to identify the optimal design and operating conditions of serpentine separation microchannels.

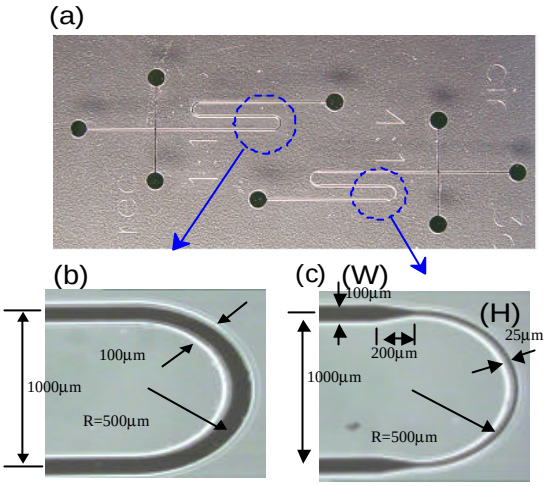

Figure 1: (a) Photograph of serpentine U-shaped separation channels, (b) detailed view of channel with bend ratio of 1, and (c) detailed view of channel with bend ratio of 4

Experiment section

Fabrication Process. The microchip substrates used in the current experimental study were formed by cutting polished soda-lime glasses for SDN-LCD displays (300 x 400 x 1.1 mm^3, G-Tech Opto-electronics Corporation, Taiwan) into plates measuring 30 mm x 80 mm. Figure 2 presents a simplified overview of the fabrication process which was used to form the planar microfluidic channels on the glass substrates [7]. Initially, the glass substrates were cleaned thoroughly by placing them in a boiling Piranha solution (H_2SO_4 (98%):H_2O_2 (30%)= 3:1, volume ratio) for 10 minutes. Rather than using a time-consuming vacuum deposition process to fabricate the mask required to etch the plates in an HF-based etchant, this study applied a 3-µm thick AZ4620 (Clariant Corp., USA) photoresist layer as the masking material in the wet chemical etching process. As shown in Figure 2(a), a standard lithography process was used to generate the required configuration of the microchannels. Note that the width of these microchannels was 100 µm. The patterned substrates were then etched for 45 minutes in a 6:1 BOE (Buffered Oxide Etchant, J. T. Baker, USA) bath, which was agitated ultrasonically, to form 40-µm-deep microfluidic trenches (Figure 2(b)). As shown in Figure 2(c), the PR layer was then removed. Meanwhile, via holes were drilled in simple 30 mm x 80 mm glass plates, then cleaned in a boiling Piranha solution (Figure 2(d)). The two glass flats were then carefully aligned and made to cling to each other using DI water, as shown in Figure 2(e), and finally the two plates were thermally bonded in a sintering oven at 580 °C for 10 minutes (Figure 2(f)).

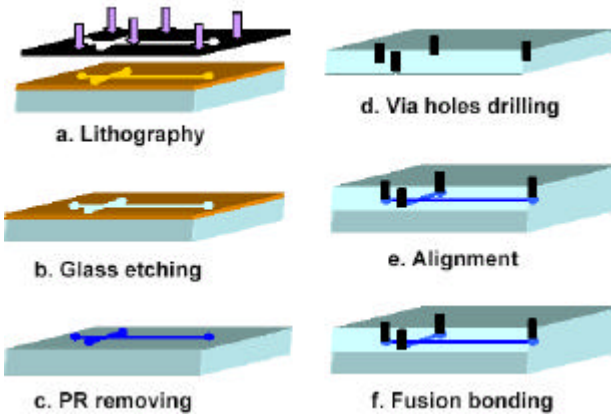

Figure 2: Fabrication of glass-based microfluidic chip.

Instrumentation. The microfluidic chip performance was monitored using a laser-induced fluorescence (LIF) technique. The fluid sample manipulations were observed by mercury lamp induced fluorescence using a charge-coupled device for imaging purposes. Under this arrangement, the experimental images were captured by an optical microscope, filtered spectrally (550 nm cut-on), and then measured using the CCD device. The voltage switching apparatus was computer-controlled using an in-house program developed with Labview software. Finally, the emitted optical signals were detected using an APD module (Avalanche Photo-Diode, C5640-01, Hamamatsu, Japan) and a PMT (Photo Multiplier Tube, R928, Hamamatsu, Tokyo, Japan) module.

Analytes. The sample considered in the electroosmotic flow study consisted of 10^{-4} M Rhodamine B fluorescent dye. Meanwhile, 1 mM $Na_2B_4O_7 \cdot 10H_2O$ with a pH value of 9.2 was utilized as the buffer solution throughout. Regarding the electrophoresis flow studies, the DNA sample used in the straight separation channel investigation was a 100-bp DNA ladder consisting of ten fragments, i.e. 100, 200,

ISSN: 1727-1983

300, 400, 500, 600, 700, 800, 900 and 1000 base pairs (bp). A 0.5μl DNA sample with a concentration of 1μg/ml was injected into a conventional cross-type CE chip. Detection of the 100-bp DNA ladder was conducted using a CE buffer of 1.5% HPMC (Hydroxypropyl Methyl Cellulose, Acros Organics, Belgium) in TBE (tris-borate-EDTA, Sigma-Aldrich, USA) with 1μM of TO-PRO-3 (Molecular probes, USA) fluorescent dye. In the detection procedure, a voltage of 180V (300 V/cm) was applied to the buffer channel causing the sample to be driven across the intersection of the channels. Through the appropriate application of a high voltage (1.08 kV, 300 V/cm) to the separation channel, a small amount of the sample was injected into the separation channel. The separated DNA fragments were then detected using a fluorescence microscope (BX60, Olympus, Japan). In the detection process, the excitation light was generated using a mercury lamp, filtered by a 530-550 band pass filter, and then focused on the detection spot of the CE chip through the fluorescence microscope. The induced fluorescence from the DNA sample was filtered using a 580 nm high pass filter and then detected through a fluorescence microscopy technique using a photomultiplier tube (R928, Hamamatsu, Japan).

Formulation and numerical method

Regarding the numerical simulation of electroosmotic flows, the current authors have previously developed physical models based on (a) the Poisson equation for the electrical potential and zeta potential, (b) the Nernst—Planck equations for the ionic concentration, (c) the full Navier—Stokes equations modified to include the effects of the body force due to the electrical and charge densities and (d) a concentration equation for the sample plug distribution. The detailed expressions of the governing equation, the initial conditions, and the boundary conditions are provided in reference [8].

$$\nabla^2 y = -\frac{k^2}{2} r_e \tag{1}$$

$$\frac{\partial n_i}{\partial t} + \vec{u}\nabla n_i = \frac{1}{Sc\,\mathrm{Re}}\nabla^2 n_i + \frac{1}{Sc\,\mathrm{Re}}\left[\nabla\left(n_i \nabla y\right)\right] \tag{2}$$

$$\nabla \cdot \vec{u} = 0 \tag{3}$$

$$\frac{\partial \vec{u}}{\partial t} + \vec{u} \cdot \nabla \vec{u} = -\nabla p + \frac{1}{\mathrm{Re}}\nabla^2 \vec{u} - G_x r_e \nabla y \tag{4}$$

$$\frac{\partial C}{\partial t} + \vec{u} \cdot \nabla C = \frac{1}{Sc\,\mathrm{Re}}\nabla^2 C \tag{5}$$

Results and discussion

In the current study, the separation channels incorporated 180^0 turns of various bend ratios. The key geometric variables of the turns are indicated in Figure 1(c). The microchannel widths in the separation and curved portions are denoted by *W* and *H*, respectively, and the ratio of these widths, i.e. *W/H*, is defined as the bend ratio, *n*.

Traditional straight separation channel. Fluid flow through straight microchannels has been thoroughly investigated both experimentally and theoretically in previous studies and the results are readily available in the published literature. Electrophoresis separation is traditionally performed in a straight separation channel since the resulting sample band in the detection area has a better shape for resolution purposes. In this type of separation microchannel flow, an applied electric field acts on the net fluid charge near the wall and produces a body force which drives fluid motion. Figure 3 presents an electropherogram generated from an image collected at the detection area of the straight separation channel (3cm). In the present experiment, the 100-bp DNA ladder sample consisted of ten fragments of 100, 200, 300, 400, 500, 600, 700, 800, 900 and 1000 base pairs (bp). A DNA sample of volume 0.5 μl and concentration 1μg/ml was loaded in a conventional cross-type CE chip, and an injection voltage of 180V (300 V/cm) was then applied for a duration of 30 sec. Subsequently, a separation voltage of 1.08 kV (300 V/cm) was applied for a duration of 2 min. The separation result for the 100-bp DNA ladder sample presented in Figure 3 reveals the presence of ten obvious peaks. The experimental results provided in this figure serve as a benchmark against which to compare the results of the subsequent separation experiments conduced with serpentine U-shaped microchips of different bend ratios.

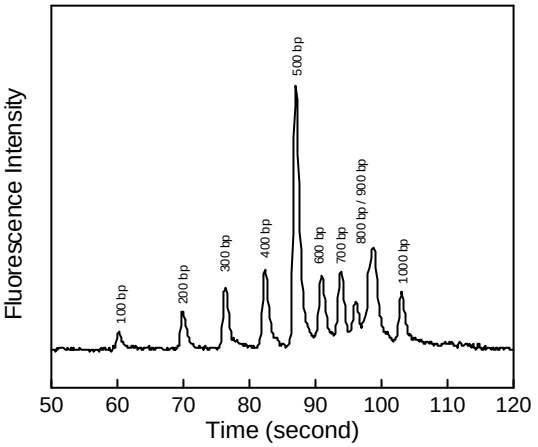

Figure 3: Electropherogram of separation results for 100-bp DNA ladder sample generated from image collected at detection area of straight separation channel (3cm) with voltage 1.08 kV (300 V/cm).

Bend ratio of 1. In electrophoresis separation, flow vorticity effects influence the shape of the velocity profile, and hence the efficiency of the separation. The flatter the velocity profile, the better the separation efficiency. It is essential to control the velocity distribution in the cross-section of the turn in serpentine separation channels. The bend ratio is known to be a key parameter in controlling this characteristic. Figure 4 presents the velocity profiles across the microchannel width at different cross-sections of the curved area of the

ISSN: 1727-1983

microchannel with a bend ratio of 1.

It is observed that the velocity profile is uniform and flat in the region immediately before the curved portion of the separation channel (*a-a* cross-section). As the fluid enters the curved separation channel (*b-b*), the average velocity in the inner channel area (from 0~50 μm) is found to be 1.15 times that of the average velocity in the outer channel (from 50~100 μm). Meanwhile, at the *c-c* section, the inner velocity is approximately 1.35 times that of the outer channel. Hence, the results provide clear evidence of the "racetrack" effect as the fluid flows around the U-bend region of this particular microchannel.

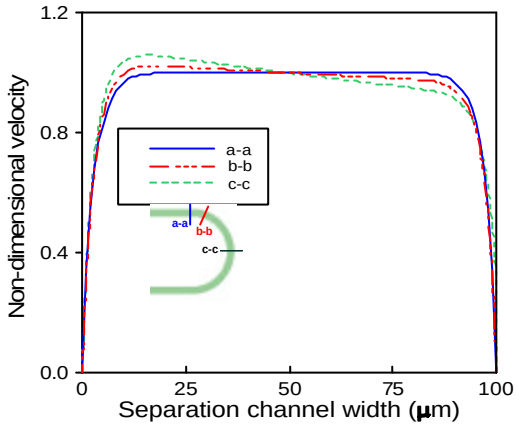

Figure 4: Comparison of velocity profiles at different cross-sections for bend ratio of 1.

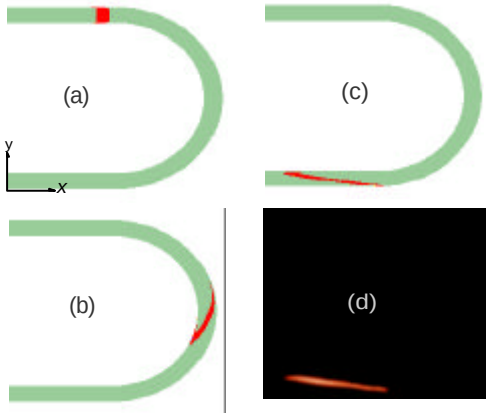

Figure 5: Sequence of band concentration distributions in U-shaped separation channel for bend ratio of 1.

Figure 5 presents the numerical simulation and experimental results for the normal progression of a band distribution through a curved separation channel with a bend ratio of 1. Figures 5(a)-5(c) indicate that the racetrack effect causes the band distribution to become skewed and distorted as it travels around the 180^0 turn. Figure 5(d) shows the experimentally obtained CCD image of the band distribution after the 180^0 turn. It is noted that this image is in good agreement with the equivalent numerical result of Figure 5(c).

Figure 6 presents an electropherogram for the separation of the 100-bp DNA ladder for a separation voltage of 1.08 kV (300 V/cm) and a bend ratio of 1. For the same sample in a conventional separation channel, Figure 3 has shown ten obvious peaks corresponding to the individual DNA fragments. However, in the present case, it can be seen that the resolution is rather poor, and hence it is difficult to identify precisely the peaks corresponding to the 600, 700 and 800-bp fragments. Therefore, it is clear that the racetrack effect induces a significant dispersion of the sample band in a curved separation channel with a bend ratio of 1.

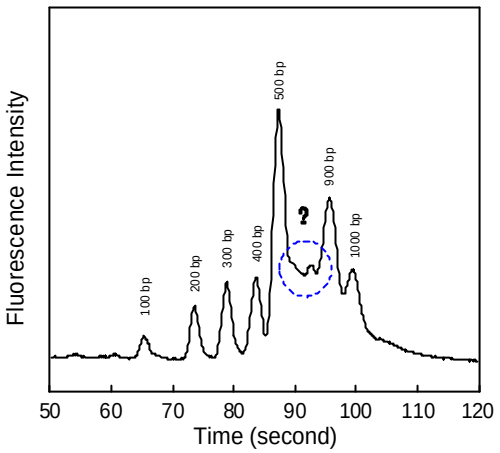

Figure 6: Electropherogram of separation results for 100-bp DNA ladder sample generated from image collected at detection area of serpentine U-shaped separation channel (3cm) with voltage 1.08 kV (300 V/cm) and bend ratio of 1.

Bend ratio of 2. The second experiment uses a fluid with the same physical properties as those described in the previous case. Figure 7 presents the velocity profiles at different cross-sections of a curved microchannel with a bend ratio of 2. In this figure, it can be seen that the velocity profile has a slightly concave shape prior to entering the curved region of the separation channel (*a-a* cross-section) since the transition from a larger cross-sectional area to a smaller area establishes a flow resistance. When the fluid enters the curved separation channel (*b-b* cross-section), the average velocity in the inner channel (from 0~50 μm) is found to be 1.01 times that of the outer channel (from 50~100 μm), while at cross-section *c-c*, the inner channel velocity is 1.10 times that of the velocity in the outer channel. Therefore, the present results suggest that a bend ratio of 2 has little effect in reducing the racetrack effect.

Figure 8 presents the numerical simulation and experimental results for the band distribution at various locations around the turned separation channel with a bend ratio of 2. Figures 8(a)-8(c) reveal that the band becomes slanted and distorted as it travels around the 180^0 turn. Meanwhile, Figure 8(d) shows the experimentally obtained CCD image results of the band distribution after the 180^0 turn. It is observed that the image is similar to the numerical simulation results of Fig. 8(c). The normalized induced

ISSN: 1727-1983

variance for the turn in Fig. 8(c) and Fig. 8(d) are found to be $(\sigma/a)^2 \approx 0.9124$ and 0.9386 , respectively. Figure 9 shows an electropherogram for the separation of the 100-bp DNA ladder for a separation voltage of 1.08 kV (300 V/cm) and a bend ratio of 2. It is noticeable that the identity of the 700 and 800-bp peaks are unclear. Furthermore, there is no perceptible improvement in the resolution compared to the case of a bend ratio of 1.

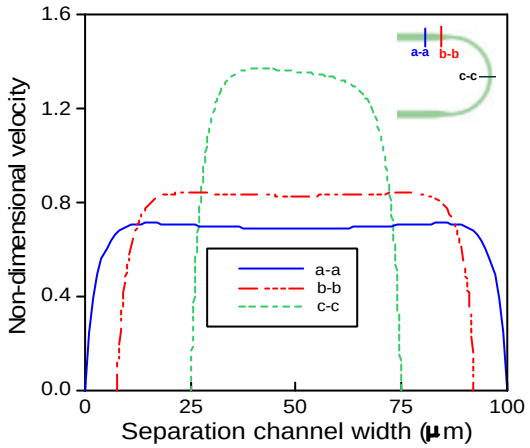

Figure 7: Comparison of velocity profiles at different cross-sections for bend ratio of 2

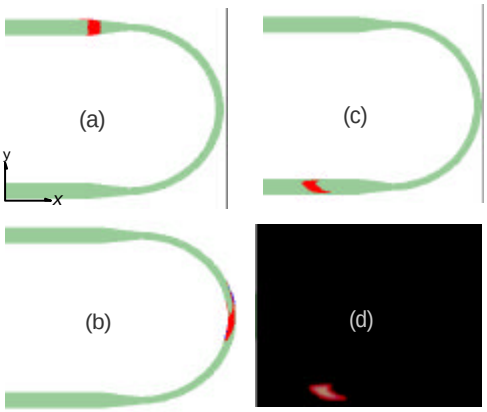

Figure 8: Sequence of band concentration distributions in U-shaped separation channel for bend ratio of 2

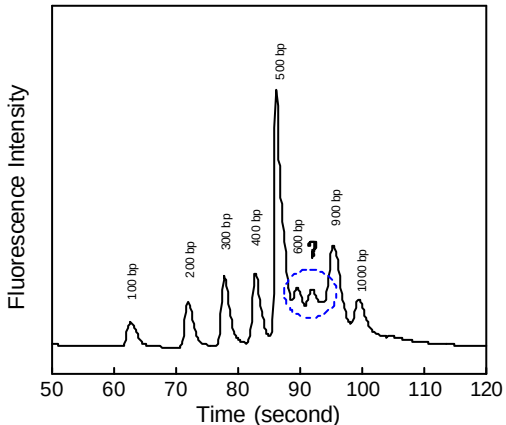

Figure 9: Electropherogram of separation results for 100-bp DNA ladder sample generated from image collected at detection area of serpentine U-shaped separation channel (3cm) with voltage 1.08 kV (300 V/cm) and bend ratio of 2.

Bend ratio of 4. The intention of this particular experiment is to correct the tilt and distortion of the band shape by adopting a higher bend ratio of 4. Figure 10 presents the velocity profiles at difference cross-sections around the curved portion of the microchannel. It can be seen that the velocity profile has a concave shape both prior to entering the curved region (*a-a*) and within the curved region itself (*b-b*) as a result of the greater flow resistance generated by the larger bend ratio (separation channel width: turn channel width = 100 μm: 25 μm = 4:1). As the fluid flows through the turned separation channel, the ratio of the average velocity in the inner channel (from 0~50 μm) to that in the outer channel (from 50~100 μm) at cross-sections *b-b* and *c-c* is 1:1. Therefore, it is clear that a bend ratio of 4 has a significant effect in reducing the racetrack effect within the turned separation channel.

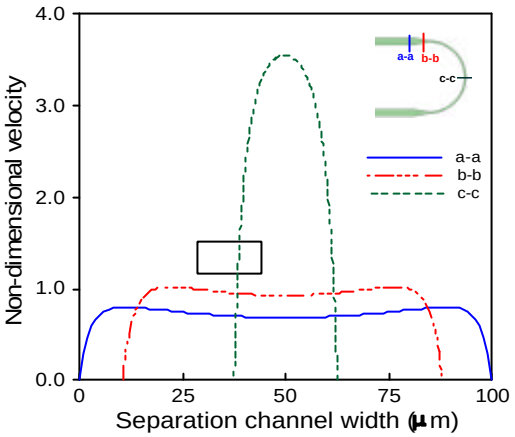

Figure 10: Comparison of velocity profiles at different cross-sections for bend ratio of 4.

The benefit of the optimized low-dispersion turn is illustrated in Figure 11, which reveals a satisfactory band shape in both the numerical and experimental results. The figure demonstrates a significant reduction in the racetrack effect. It can be seen that the band which emerges from the turn is orthogonal to the separation channel walls. The induced variance for this low-dispersion turn of numerical simulation and experiment are only $(\sigma/a)^2 \approx 0.00214$ and 0.00348, i.e. more than 3 orders of magnitude lower than the variances calculated for the previous cases (bend ratios of 1 and 2). Figure 12 presents an electropherogram of the 100-bp DNA ladder generated from an image collected at the detection area for a separation voltage of 1.08 kV (300 V/cm) and a bend ratio of 4. This figure clearly shows that the resolutions of the 800-bp and 900-bp peaks have been improved in the detection area. These results confirm that the dispersive effect is diminished in the 180^0 turn separation channel when the bend ratio is 4.

Figure 13 presents an electropherogram generated from an image collected at the detection area of a multi-turned separation channel (eight turns, total separation length 7 cm) with a separation voltage of 2.28 kV (300 V/cm) and a bend ratio of 4 In this case, the

ISSN: 1727-1983

chip measures 1.5 cm × 2.5 cm. The results for the 100-bp DNA ladder demonstrate that this multi-turned separation channel provides a high separation performance (i.e. the induced variance is as small as that achieved in a 7cm straight separation channel). It is clear that an appropriate bend ratio design has a significant influence in improving the separation detection performance within serpentine U-shaped separation channels.

Conclusion

This study has presented an experimental and numerical investigation into the development of microfabricated chemical analysis devices which are obliged to use serpentine separation channels to satisfy device miniaturization requirements, but which must also maintain an acceptable degree of electrophoresis performance. The present numerical model provides a useful tool for simulating the turn-induced diffusive and dispersive spreading of a species band as it flows through serpentine separation channels. This study has performed the experimental separation of 100-bp DNA ladder samples in order to explore the effects of the bend ratio on the separation performance. The results have shown that band tilting is corrected and the racetrack effect is reduced when a bend ratio of 4 is specified for the curved region of the microchannel. Qualitatively, it has been verified that the low-dispersion turn with a bend ratio of 4 results in an induced variance which is 3 orders of magnitude less than that for a uniform turn (bend ratio 1). Furthermore, the present investigations have demonstrated that the use of a 7 cm multi-turned U-shaped separation channel configured within a 1.5 cm × 2.5 cm area is capable of a high performance, i.e. 99 % of that obtained using a conventional straight separation channel of equivalent length. The present results provide a valuable reference for the future development of optimized DNA separation channels with enhanced performance.

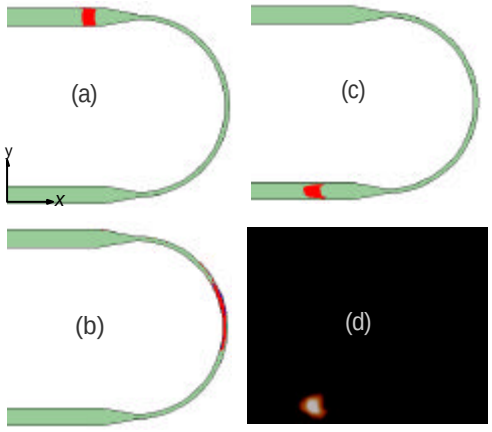

Figure 11: Sequence of band concentration distributions in U-shaped separation channel for bend ratio of 4.

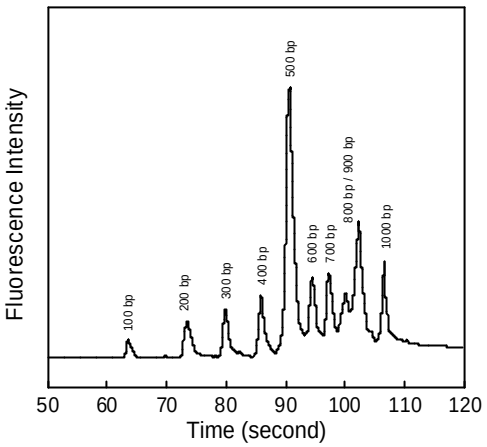

Figure 12: Electropherogram of separation results for 100-bp DNA ladder sample generated from image collected at detection area of serpentine U-shaped separation channel (3cm) with voltage 1.08 kV (300 V/cm) and bend ratio of 4.

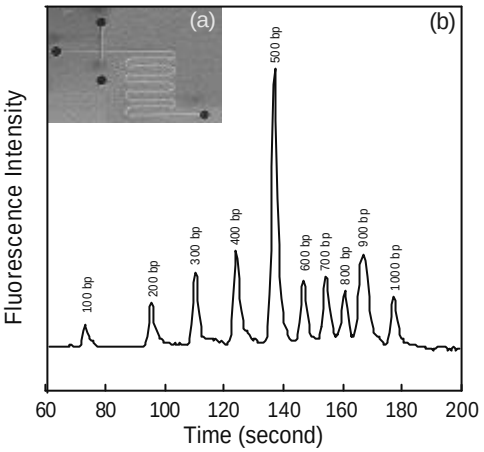

Figure 13: (a) Photographs of multi-turn U-shaped separation channels (total separation channel length 7 cm), and (b) Electropherogram of separation results for 100-bp DNA ladder sample generated from image collected at detection area of serpentine U-shaped separation channel (7cm) with voltage 2.28 kV (300 V/cm) and bend ratio of 4.

Acknowledgment

This study was supported by the National Science Council of Taiwan through the grant number NSC94-2320-B-020-001.

References

[1] Culbertson C., Ramsey R. and Ramsey J. M., (2000): 'Electroosmotically induced hydraulic pumping on microchips: differential ion transport', *Analytical Chemistry*, 72, pp.2285-2291.

[2] Gao J., Yin X. F. and Fang Z. L., (2004): 'Integration of single cell injection, cell lysis, separation and detection of intracellular constituents on a microfluidic chip', *Lab on a Chip*, 4, pp. 47-52.

ISSN: 1727-1983

[3] Fu L. M., Yang R. J., Lin C. H., Pan Y. J. and Lee G B., (2004): 'Electrokinetically driven micro flow cytometers with integrated fiber optics for on-line cell/particle detection' *Analytica Chimica Acta,* 507, pp. 163–169.

[4] Erickson D. and Li D., (2004): 'Integrated microfluidic devices', *Analytica Chimica Acta,* 507, pp. 11–26.

[5] Culbertson C. T. and Jacobson S. C., (1998): 'Dispersion sources for compact geometries on microchips', *Analytical Chemistry,* 70, pp. 3781-3789.

[6] Molho I., Herr A. E., Mosier B. P., Stantiago J. G., Kenny T. W., Brennen R. A., Gordon G B. and Mohammadi B., (2001): 'Optimization of turn geometries for electrophoresis microchip', *Analytical Chemistry,* 73, pp. 1350-1360.

[7] Lin C. H., Lee G. B., Lin Y H. and Chang G. L, (2001): 'A fast prototyping process for fabrication of microfluidic systems on soda-lime galss', *J. Micromech. Microeng.,* 11, pp. 726-732.

[8] Fu L. M. and Yang R. J., (2003): 'Low voltage-driven control in electrophoresis microchips by moving electric field', *Electrophoresis* 24, pp. 1253-1260.

ISSN: 1727-1983